2021 43rd Annual International Conference of the
IEEE Engineering in Medicine & Biology Society (EMBC)
Oct 31 - Nov 4, 2021. Virtual Conference

# Placental Super Micro-vessels Segmentation Based on ResNeXt with Convolutional Block Attention and U-Net

*Minsi Chen[1], Cheng Zhao[1], Xiaoxian Tian[2], Yujian Liu[1], Tianfu Wang[1*], Baiying Lei[1*]*
[1]School of Biomedical Engineering, Shenzhen University,National-Regional Key Technology Engineering Laboratory for Medical Ultrasound,Guangdong Key Laboratory for Biomedical Measurements and Ultrasound Imaging, Shenzhen, China.
[2]Department of Ultrasound, Guangxi Maternal and Child Health Hospital, Nanning, China.
(*Email:{leiby@szu.edu.cn, tfwang@szu.edu.cn})

**Abstract–Accurate placenta super micro-vessels segmentation is the key to diagnose placental diseases. However, the current automatic segmentation algorithm has issues of information redundancy and low information utilization, which reduces the segmentation accuracy. To solve this problem, we propose a model based on ResNeXt with convolutional block attention module (CBAM) and UNet (RC-UNet) for placental super micro-vessels segmentation. In the RC-UNet model, we choose the UNet as the backbone network for initial feature extraction. At the same time, we select ResNeXt-CBAM as the attention module for feature refinement and weighting. Specifically, we stack the blocks of the same topology following the split-transform-merge strategy to reduce the redundancy of hyper-parameter. Moreover, we conduct CBAM processing on each group of the detailed features to get informative features and suppress unnecessary features, which improve the information utilization. The experiments on the self-collected data show that the proposed algorithm has better segmentation results for anatomical structures (umbilical cord blood (UC), stem villus (ST), maternal blood (MA)) than other selected algorithms.**

**Index Terms—**Placental super micro-vessels segmentation, ResNeXt network, UNet, Convolutional block attention module.

## I. Introduction

The nutria delivery of the placenta to the fetus is dependent on the abundant placenta super micro-vessels [1]. Its shape and density reflect the nutrient supply of the placenta and the development of the fetus [2]. To monitor the health of the fetus and evaluate the growth of the fetus [3-5], it is necessary to carry out related quantitative evaluations of super capillaries. The premise of the evaluation is to accurately segment the placenta super micro-vessels (umbilical cord blood (UC), stem villus (ST), maternal blood (MA)). The visualization results of Fig.1 show that UC, ST, and MA can be segmented and distinguished accurately.

At present, due to the low resolution of ultrasound imaging and the difference in doctors' subjective observation, there are many differences in the measured placental index, which causes great difficulties in the evaluation of placenta super micro-vessels. Therefore, it is desired to develop an objective and automatic method to evaluate placenta function.

To improve the accuracy of image segmentation, many scholars increase the neural network's depth to improve performance [6, 7], but it has the issues of increasing the amount of calculation and the difficulty of optimization. To solve it, grouped convolutions [8] divide the convolution kernel into different groups and perform convolution operations separately to increase the computation efficiency. In recent years, ResNeXt [9] and Res2Net [10] apply the idea of grouped convolutions, which significantly improves performance without increasing computing costs, exhibits excellent robustness in computer vision tasks [11-13].

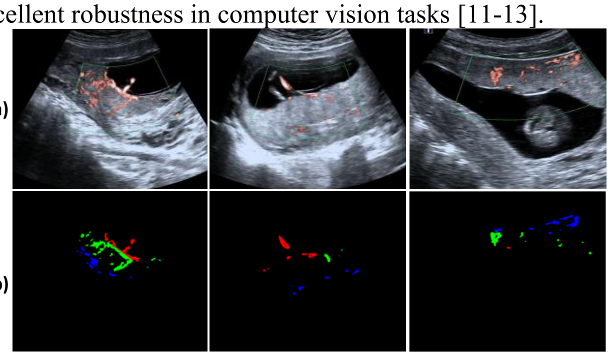


Fig.1. (a) Prenatal ultrasound image. (b) Segmentation of placental super micro-vessels. The red is UC, which is attached to the surface of the placenta and connected to the fetus. The green is the ST, usually longitudinal, which can exchange maternal blood and umbilical cord blood. The blue is MA, which exchanges blood inside and outside the placenta.

Apart from increasing the neural network's depth, some scholars have proposed to improve the segmentation accuracy by introducing attention mechanism [14]. SE-Net [15] introduces a compact module to exploit the inter-channel relationship. Besides, Block attention module (BAM) [16] and convolutional BAM (CBAM) [17] employ spatial and channel attention modules, which improve the performance of interest.

For this reason, we propose a model based on ResNeXt-CBAM and UNet [18] to segment placenta super micro-vessels accurately. We first send prenatal ultrasound images into the UNet to extract the initial feature. Then, in the ResNeXt-CBAM network, we employ a split-transform-merge strategy to reduce the redundancy of hyper-parameter. To set a larger weight for the region of interest, we use the CBAM module in the feature propagation to focus on feature extraction. Our model takes advantage of CBAM, ResNeXt, and UNet. As far as we know, we are the first to study automatic placenta super micro-vessels segmentation.

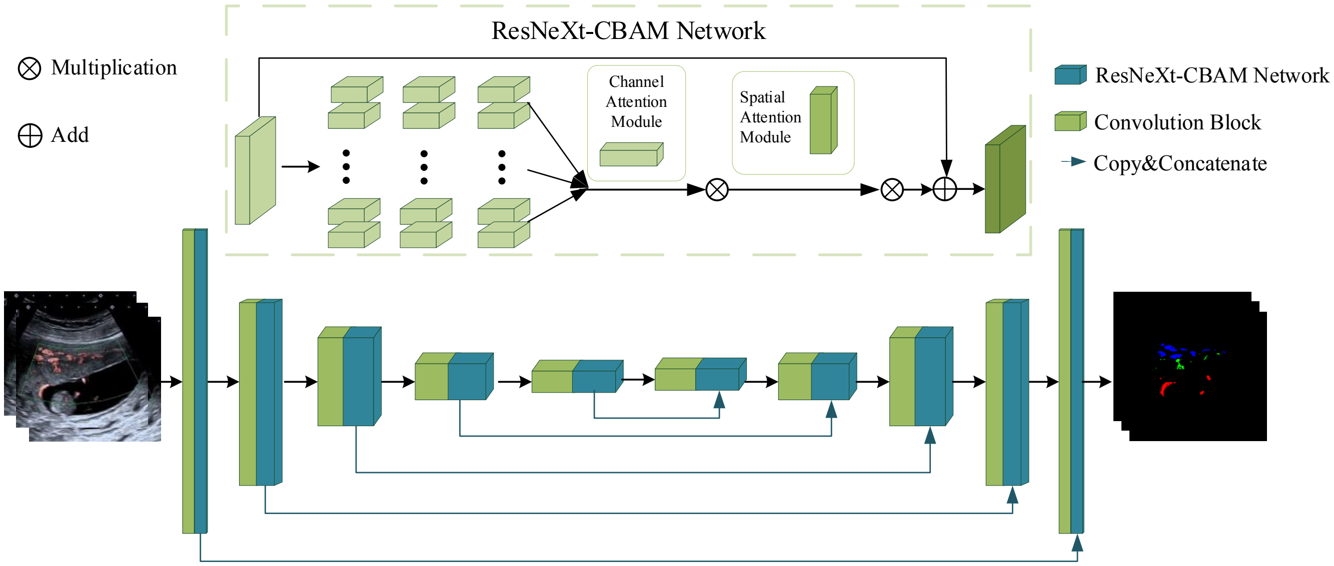


Fig.2. RC-UNet segmentation network.

We present a new deep neural network model by modifying the ResNeXt-CBAM and UNet architectures and adopt it for placenta super micro-vessels segmentation. The designed RC-UNet model shows promising results in our comparative experiments.

## II. Methodology

We select UNet as the backbone network and use the ResNeXt-CBAM network for feature extraction. Fig. 2 shows the detailed structure. The overall process of the ResNeXt-CBAM network is as follows.

### *A. ResNeXt-CBAM network*

ResNeXt-CBAM network: In the ResNeXt-CBAM network, the ResNeXt network follows the split-transform-merge strategy to extract the features of each layer. The final outputs are aggregated by summation. We add the CBAM module after the ResNeXt network. The output of ResNeXt network is an intermediate feature map $\boldsymbol{F} \in R^{c \times h \times w}$, CBAM infers a channel feature map $\boldsymbol{Q_c} \in R^{1 \times 1 \times c}$, and a spatial feature map $\boldsymbol{Q_s} \in R^{1 \times w \times h}$. The whole process can be described by the following formula:

$$\boldsymbol{F_1} = \boldsymbol{Q_c}(\boldsymbol{F}) \otimes \boldsymbol{F}\,, \qquad (1)$$

$$\boldsymbol{F_2} = \boldsymbol{Q_s}(\boldsymbol{F_1}) \otimes \boldsymbol{F_1}\,, \qquad (2)$$

where $\otimes$ means element-wise multiplication, $\boldsymbol{F}$ is the input feature map obtained by ResNeXt network, $\boldsymbol{F_2}$ is the final output of the CBAM module, $\boldsymbol{Q_c}$and $\boldsymbol{Q_s}$ denote the channel and spatial attention operations, respectively. The overall implementation process of the channel attention module and the spatial attention module is as follows:

Channel attention module: The channel attention module exploits the inter-channel relationship of features and generates a channel attention map. This channel weighted module has two branches, one uses the global max-pooling, and another branch adopts global average-pooling followed by projection using a shared multi-layer perceptron (MLP) with one hidden layer. The final feature of channel attention module is obtained by the sigmoid function, which is shown in Fig.3.

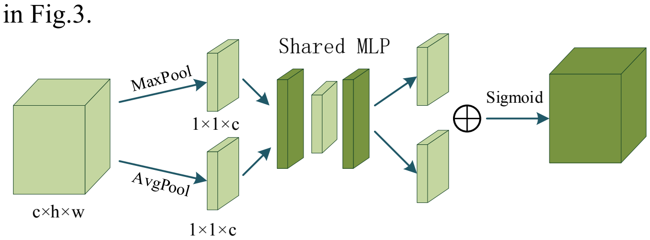


Fig.3 Channel attention module.

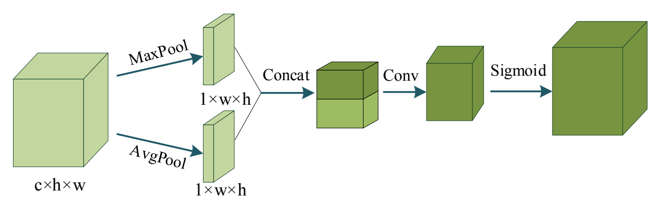


Fig.4 Spatial attention module.

Spatial attention module: This module also has two branches. One branch performs global max-pooling in the channel direction, while the other branch performs global average-pooling. We concatenate the two branch results to generate an efficient feature descriptor. After that, a convolution operation (the size of the convolution kernel is 7×7) reduces the number of channels to one. The final feature is also obtained by the sigmoid function, which is shown in Fig.4.

### *B. Network Architecture*

Our segmentation network's main framework is UNet. To extract the distinctive features of different layers, we add the CBAM to UNet. In the ResNeXt-CBAM network, we follow the split-transform-merge strategy and stack the blocks of the same topology for feature extraction. Therefore, the overall implementation process is as follows: 1) We use the UNet to extract the initial features. 2) We choose the ResNeXt-CBAM network for feature extraction. 3) We concatenate the salient features of the encoder with the corresponding up-sampling features (obtained by UNet) in the corresponding layer of the decoder. 4) The corresponding layer feature is obtained by convolution operation, and the final segmentation feature is obtained by the softmax function.

### C. Loss Function

In this paper, we choose binary cross-entropy and dice loss functions to construct a hybrid objective function for optimizing network training. The objective function is as follows:

$$L_{sum} = \alpha L_{bce} + \beta L_{Dice}, \quad (3)$$

where $\alpha$ = 0.5, $\beta$ = 0.5, $\alpha$ and $\beta$ are the weight parameters used to balance the two branches.

The binary cross-entropy is then defined as follows:

$$L_{bce} = \sum_i y_i \log O_i + (1 - y_i)\log(1 - O_i), \quad (4)$$

where $O_i \in \{1,0\}$ is the $O^{th}$output of the last network layer passed through a sigmoid nonlinearity.

Dice loss can be expressed as:

$$L_{Dice} = -\frac{2\sum_i O_i y_i}{\sum_i O_i + \sum_i y_i}, \quad (5)$$

where $y_i \in \{0,1\}$ is the corresponding label.

## III. Experiments and Results

### A. Experimental setup

The data used in this paper are ultrasound images collected from Guangxi Maternal and Child Health Hospital in 2019. Our data comes from 155 patients. There are 890 ultrasound images in total. We randomly divide the dataset into training and testing set in a ratio of 4:1. The ground truth segmentation was annotated by three experienced Sonographers.

To keep the fairness of all experiments, the setting in all experiments is consistent. We use Adam optimizer and the initial learning rate is set to $10^{-4}$ and decreased by a factor of 0.1 every 10 epoch. The training epoch is 60, batch size is 4.

### B. Segmentation results

In this subsection, we perform the ablation and comparison experiments to verify the effectiveness of the proposed method, which are detailed in Table 1 and Table 2.

In Table 1, we compare the influence of ResNeXt and ResNeXt-CBAM on the UNet network designed to enhance the segmentation performance. For UNet, the experimental results show that adding the ResNeXt-CBAM network will significantly increase or be similar to the three evaluation indicators in terms of the mean value compared with adding ResNeXt. Moreover, it can be seen that the benefits of this improvement are more obvious on the shallower ResNeXt network.

In Table 2, we select the ResNeXt-SE network to replace the ResNeXt-CBAM network and use Res2Net-CBAM to replace ResNeXt-CBAM for ablation experiments. The results show that ResNeXt-CBAM performs much better than other networks for segmenting the placental super micro-vessels.

### D. Visualization results

Fig. 5 shows the segmentation results of different methods. UC blood, ST, and MA blood are represented by red, green and blue, respectively. From the visualized segmentation results of each method, the network with the ResNeXt-CBAM network is better than the network with the ResNeXt-SE network. For ResNeXt-CBAM and Res2Net-CBAM, assigning ResNeXt-CBAM network is better than using Res2NeXt-CBAM network for the placental super micro-vessels segmentation. This verifies our conjecture that the RC-UNet network has an excellent prospect on the placental super micro-vessels segmentation.

## IV. Conclusion

In this paper, we propose a RC-UNet model to accurately segment placental super micro-vessels from ultrasound images. It includes two sub-sections: ResNeXt-CBAM network utilizes channel attention and spatial attention to reduce information loss and uses grouped convolution to improve operational efficiency.

**Table 1.** Segmentation results of different methods.

| Architecture | Dice | | | | Precision | | | | Recall | | | |
|---|---|---|---|---|---|---|---|---|---|---|---|---|
| | UC | ST | MA | mean | UC | ST | MA | mean | UC | ST | MA | mean |
| UNet | 0.783 | 0.677 | 0.764 | 0.741 | 0.817 | 0.730 | 0.800 | 0.752 | 0.830 | 0.701 | 0.815 | 0.782 |
| ResNeXt50-UNet | 0.784 | 0.684 | 0.773 | 0.747 | 0.805 | 0.719 | **0.831** | 0.785 | 0.849 | **0.727** | **0.889** | 0.788 |
| ResNeXt50-CBAM network with UNet | **0.827** | 0.677 | 0.791 | **0.765** | **0.820** | **0.752** | 0.809 | **0.794** | **0.910** | 0.694 | 0.839 | **0.815** |
| ResNeXt101-CBAM network with UNet | 0.778 | **0.696** | **0.800** | 0.758 | 0.812 | 0.743 | 0.825 | 0.794 | 0.845 | 0.713 | 0.831 | 0.796 |

**Table 2.** Ablation experiments with and without CBAM module or ResNeXt50 network on UNet

| Architecture | Dice | | | | Precision | | | | Recall | | | |
|---|---|---|---|---|---|---|---|---|---|---|---|---|
| | UC | ST | MA | mean | UC | ST | MA | mean | UC | ST | MA | mean |
| ResNeXt50-SE network with UNet | 0.794 | **0.685** | 0.782 | 0.754 | 0.802 | 0.739 | 0.815 | 0.785 | 0.855 | **0.704** | 0.815 | 0.791 |
| ResNeXt50-CBAM network with UNet | **0.827** | 0.677 | **0.791** | **0.765** | **0.820** | **0.752** | 0.809 | **0.794** | **0.910** | 0.694 | **0.839** | **0.815** |
| Res2Net50-CBAM network with UNet | 0.738 | 0.632 | 0.775 | 0.715 | 0.790 | 0.728 | **0.823** | 0.780 | 0.772 | 0.623 | 0.779 | 0.725 |

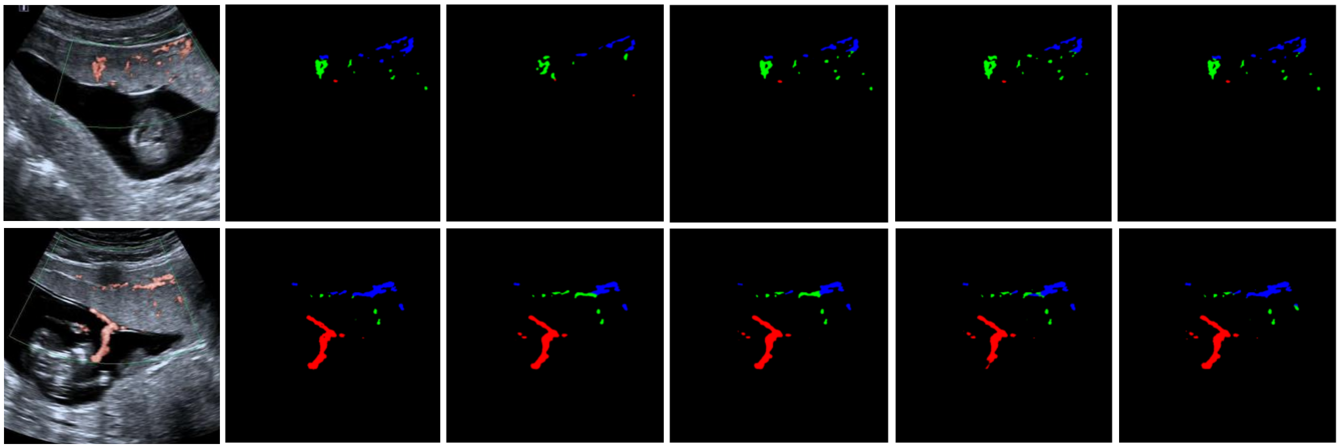

Raw image | Ground truth | Res2Net50-SE network with UNet | Res2Net50-CBAM network with UNet | ResNeXt50-SE network with UNet | ResNeXt50-CBAM network with UNet

Fig. 5. Visualized segmentation results of different methods.

Our model combines the advantages of ResNeXt-CBAM and UNet, which significantly improves the accuracy of placental super micro-vessels segmentation. We add the ResNeXt and ResNeXt-CBAM network into the UNet respectively to make comparative experiments. Moreover, we select ResNeXt-SE network to replace the ResNeXt-CBAM network and the Res2Net-CBAM network replace ResNeXt-CBAM network to make two comparative experiments. Experiments show that our method performs better than other networks for segmenting the placental super micro-vessels.

## V. Compliance with Ethical Standard

The study was performed in line with the principles of the Declaration of Helsinki. Approval was granted by the Ethics Committee of Guangxi Maternal and Child Health Hospital (December 5, 2019).

## VI. Acknowledgments

This work was supported partly by National Natural Science Foundation of China (Nos.61871274, 61801305 and 81571758), National Natural Science Foundation of Guangdong Province (No. 2017A030313377), Guangdong Pearl River Talents Plan (2016ZT06S220), Shenzhen Peacock Plan (Nos. KQTD2016053112051497 and KQTD2015033016 104926), and Shenzhen Key Basic Research Project (Nos. JCYJ20170413152804728, JCYJ20180507184647636, JCYJ20170818142347251 and JCYJ20170818094109846).

## VII. References


[1] P. Haggarty, S. Allstaff, G. Hoad, J. Ashton, and D. J. P. Abramovich, "Placental nutrient transfer capacity and fetal growth," vol. 23, no. 1, pp. 86-92, 2002.

[2] T. R. H. Regnault, H. L. Galan, T. A. Parker, and R. V. Anthony, "Placental development in normal and compromised pregnancies - A review," *Placenta,* vol. 23, pp. S119-S129, Apr 2002.

[3] J. Zhang, M. Merialdi, L. D. Platt, and M. S. Kramer, "Defining normal and abnormal fetal growth: promises and challenges," *American Journal of Obstetrics and Gynecology,* vol. 202, no. 6, pp. 522-528, Jun 2010.

[4] W. E. Brenner, D. A. Edelman, and C. H. Hendricks, "STANDARD OF FETAL GROWTH FOR UNITED-STATES-OF-AMERICA," *American Journal of Obstetrics and Gynecology,* vol. 126, no. 5, pp. 555-564, 1976 1976.

[5] E. Ferrazzi, T. J. C. O. Stampalija…, and G. Reports, "Fetal Growth Restriction (FGR)—Fetal Evaluation and Antepartum Intervention," vol. 2, no. 2, pp. 112-121, 2013.

[6] A. Krizhevsky, I. Sutskever, and G. Hinton, "ImageNet Classification with Deep Convolutional Neural Networks," in *NIPS*, 2012.

[7] C. Szegedy, L. Wei, Y. Jia, P. Sermanet, and A. J. I. C. S. Rabinovich, "Going Deeper with Convolutions," 2014.

[8] A. Krizhevsky, I. Sutskever, and G. E. Hinton, "ImageNet Classification with Deep Convolutional Neural Networks," *Communications of the Acm,* vol. 60, no. 6, pp. 84-90, Jun 2017.

[9] S. Xie, R. Girshick, P. Dollar, Z. Tu, K. He, and Ieee, "Aggregated Residual Transformations for Deep Neural Networks," in *30th Ieee Conference on Computer Vision and Pattern Recognition*(IEEE Conference on Computer Vision and Pattern Recognition, 2017, pp. 5987-5995.

[10] S. Gao, M.-M. Cheng, K. Zhao, X.-Y. Zhang, M.-H. Yang, and P. H. S. Torr, "Res2Net: A New Multi-scale Backbone Architecture," *IEEE transactions on pattern analysis and machine intelligence,* 2019-Aug-30 2019.

[11] J. Donahue, Y. Jia, O. Vinyals, J. Hoffman, and T. Darrell, "DeCAF: A Deep Convolutional Activation Feature for Generic Visual Recognition," 2013.

[12] J. Long, E. Shelhamer, T. J. I. T. o. P. A. Darrell, and M. Intelligence, "Fully Convolutional Networks for Semantic Segmentation," vol. 39, no. 4, pp. 640-651, 2015.

[13] P. O. Pinheiro, R. Collobert, and P. Dollar, "Learning to Segment Object Candidates," 2015.

[14] X. Li, W. Wang, X. Hu, and J. Yang, "Selective Kernel Networks," in *2019 IEEE/CVF Conference on Computer Vision and Pattern Recognition (CVPR)*, 2020, pp. 510-519.

[15] J. Hu, L. Shen, S. Albanie, G. Sun, E. J. I. T. o. P. A. Wu, and M. Intelligence, "Squeeze-and-Excitation Networks," vol. PP, no. 99, 2017.

[16] W. S. Park J , Lee J Y , et al., "BAM: Bottleneck Attention Module," 2018.

[17] S. Woo, J. Park, J. Y. Lee, and I. S. Kweon, "CBAM: Convolutional Block Attention Module," *Springer, Cham,* 2018.

[18] O. Ronneberger, P. Fischer, and T. Brox, "U-Net: Convolutional Networks for Biomedical Image Segmentation," in *Medical Image Computing and Computer-Assisted Intervention, Pt Iii*, vol. 9351, N. Navab, J. Hornegger, W. M. Wells, and A. F. Frangi, Eds. (Lecture Notes in Computer Science, 2015, pp. 234-241.